

Formation of metastable hydrogen atoms by charge exchange of fast protons in magnesium and barium vapors

T. J. Morgan and F. Eriksen*

Department of Physics, Wesleyan University, Middletown, Connecticut 06457

(Received 6 December 1978)

The cross sections for the formation of H(2s) metastable atoms in H⁺ collisions with Mg and Ba alkaline-earth-metal vapors have been measured over the energy range 1.5–90 keV. The absolute value of the cross sections has been obtained by normalizing the present results to the cross section for H(2s) formation in Ar gas at 30 keV. In Ba, the cross section reaches a maximum value of 5.6×10^{-16} cm² at 3 keV. In Mg, the maximum value is 3.2×10^{-16} cm² and occurs at 7 keV. The measured cross sections exhibit structure at high energies which is attributed to inner-shell capture. A comparison of the present results with previous $n = 6$ electron-capture data in Mg indicates that the n^{-3} capture law is not obeyed. An analysis based on data available for 16 different collisions between H⁺ ions and ns^1 and ns^2 targets shows that the scaling law for the velocity v_m at which the single-electron-capture cross section is a maximum is not consistent with the Massey adiabatic criterion. Instead, the data are consistent with the relation $v_m \propto |\Delta E_\infty|^{1/2}$ where $|\Delta E_\infty|^{1/2}$ is the energy defect of the collision. The fraction of the neutral beam in the 2s state formed by collisions of H⁺ ions with thin targets of Mg and Ba is also reported. In Ba, the fraction is equal to 0.25 ± 0.05 at 2.0 keV and is rising at low energies. In Mg, the maximum value of the fraction is 0.13 ± 0.03 and occurs at ~ 7 keV.

I. INTRODUCTION

In this paper we present the results of a study of metastable-hydrogen-atom formation in collisions of energetic protons with magnesium and barium alkaline-earth-metal atoms. Charge-exchange collisions of this type, i.e.,



are of considerable fundamental interest and quite important in several areas of application.

The production of intense H(2s) metastable-beams is important in nuclear physics research since they can be easily nuclear-spin polarized by selective quenching of hyperfine states in electric and magnetic fields. The resulting polarized H(2s) beam can then be used to produce polarized H⁻ ions via electron-attachment collisions.^{1,2} H(2s) formation data are also needed in astrophysics research as input to cosmic-ray streaming models, which are used to interpret the origin of Lyman- α broad-emission lines in quasistellar objects.³ Timely interest in metastable-hydrogen-atom production and destruction in metal vapors also exists in the fields of metal-vapor laser development,^{4,5} controlled-thermonuclear-fusion research,⁶ and in studies of the Earth's upper atmosphere, where metal atoms have recently been detected in both the E and D layers.⁷

Stimulated by the work of Donnally *et al.*,⁸ several experimental^{9–13} and theoretical^{14–16} investigations have been carried out for reaction 1 using

cesium as a charge-exchange target. As a result of these studies, the desirability of Cs over atomic and molecular gaseous targets for the formation of low-energy ($E < 3$ keV) H(2s) metastable atoms is now well known. However, the scope of previous studies is narrow. Absolute cross sections for reaction 1 using metal-atom targets are available only for Cs over the limited energy range 0.2–3 keV. The objective of the present study is to obtain cross section data in other metal-atom targets over an extended energy range.

We have measured the cross section σ_{+m} for H(2s) formation in proton collisions with magnesium and barium atoms over the energy range 1.5–90 keV by observing the Lyman- α radiation emitted during electric field quenching of the 2s metastable atoms. The Lyman- α photons produced by the electric-field-induced $2s \rightarrow 2p \rightarrow 1s$ transition were counted downstream from the target and the absolute value of the cross section determined by normalizing the signal to the H⁺+Ar data of Bayfield at 30 keV.¹⁷ The present results are the first determination of σ_{+m} in alkaline-earth-metal vapors. Total single- and double-electron-capture cross sections for proton collisions with Mg and Ba have been reported in a separate paper.¹⁸ Combining the present results with our total single-electron transfer data (which we measured simultaneously with the 2s-state capture cross section), we have determined the metastable fraction f of the neutral beam over the energy range 2.0–90 keV. Previous measurements of f for metal-vapor targets have been limited to Cs and K for energies less than 10 keV.^{11–13,19–20}

Theoretical calculations of the cross section for electron capture into the $2s$ state in proton-metal-atom collisions have been very limited.¹⁴⁻¹⁶ Where comparisons with experimental data are available (for Cs at low energies) the agreement is not particularly encouraging. The present results provide data for assessing the reliability of extending existing high-energy theoretical models of electron-capture-into-excited-states to proton collisions with complex metal atoms.

II. EXPERIMENT

A. General description

A simplified diagram of the experimental arrangement is shown in Fig. 1. Most of the apparatus used in the present experiment has been described in detail in the report of our work on total cross sections in Mg and Ba.¹⁸ In this section a brief description of the overall apparatus and a detailed description of the Lyman- α detection system are presented. We refer the reader to Ref. 18 for a detailed description of the beam preparation, the metal-vapor target, the beam-particle detection region, and the cross section analysis.

A hydrogen-ion beam obtained from a radio-frequency ion source was accelerated to the desired energy between 1.5 and 90 keV. The beam was momentum analyzed and collimated before passage into the scattering target. The incident proton beam energy was determined by measuring the accelerator extraction voltage and adding to it a small correction to account for the existence of a plasma potential at the source. The correction was obtained from an *in situ* analysis of the beam energy as a function of the accelerator energy and ion-source parameters. The measured energy spread was ~ 80 eV and the mean energy is known to within ± 100 eV.

The scattering target is a stainless-steel cylindrical vessel with an effective target length of 5.5 cm. The cell has a 1-mm-diam entrance aperture and a 3-mm-diam exit aperture. The target was heated by two resistive heaters embedded in the stainless-steel block. The temperature was measured with two chromel-alumel

thermocouples, and the pressure in the cell obtained from P vs T data of Hultgren *et al.*²¹ The scattering cell can be used either as a gas target or as a metal-vapor target. To obtain absolute cross sections in Mg and Ba the measurements were normalized to the known cross section for H($2s$) formation in argon gas at 30 keV.¹⁷ This is accomplished by measuring the Lyman- α detection-system efficiency at 30 keV with Ar gas in the target cell. The Ar pressure was measured with a Baratron capacitance manometer. A study of the detector efficiency as a function of cell temperature was performed at constant Ar number density, and the efficiency was found to be independent of temperature over the range 300–870 K (the highest temperature used in the present work). The detection-system efficiency was measured several times during the course of the experiment (~ 4 months) and was found to change slowly and monotonically with time. The total change in detector efficiency from the beginning to the end of the experiment amounted to 25% and was taken into account in the final data analysis.

The design of the apparatus ensured that the scattered beam passed through the apparatus and was completely collected by the beam-particle detectors. To verify this, the Lyman- α signal and the beam-particle signals were measured at the lowest energy of the present experiment for several different aperture sizes at the exit of the target. No change in the cross section was observed.

B. Metastable-atom detection

The metastable hydrogen atoms were detected 45 cm downstream from the target by applying a transverse electric field of up to 700 V/cm which induced Stark mixing between the $2^2S_{1/2}$ state and the $2^2P_{1/2}$ state, and to a lesser extent between the $2^2S_{1/2}$ state and the $2^2P_{3/2}$ state. The induced mixing resulted in radiative decay of the $2^2S_{1/2}$ state to the ground state by emission of a Lyman- α photon (1216 Å). For a field of 600 V/cm the lifetime of the $2^2S_{1/2}$ state of hydrogen is reduced from the field-free two-photon-decay lifetime of 143 msec to 5 nsec.²² Consequently, essentially

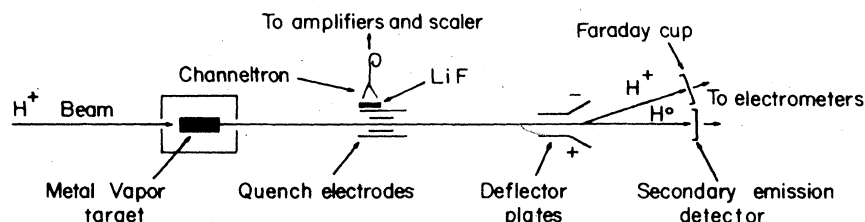


FIG. 1. Experimental arrangement.

all of the H(2s) atoms formed by electron-capture collisions in the target survive the transit from target to quench region, and decay with the emission of a Lyman- α photon in the field of view of the detector.

Because of the interference arising from the two channels $2^2S_{1/2} - 2^2P_{1/2}$ and $2^2S_{1/2} - 2^2P_{3/2}$, the Lyman- α radiation emitted in the quench region has a polarization which is dependent on the strength of the field and a corresponding electric dipole angular anisotropy given by

$$I(\theta) = \frac{3}{4}(I_0/\pi)(1 - P \cos^2\theta)/(3 - P). \quad (2)$$

In this expression I_0 is the total intensity of quench radiation, θ is the viewing angle relative to the electric field, and P is the polarization fraction defined by

$$P = (I_{\parallel} - I_{\perp}) / (I_{\parallel} + I_{\perp}), \quad (3)$$

where I_{\parallel} and I_{\perp} are the radiation intensities, viewed at $\theta = 90^\circ$, with electric field vectors parallel and perpendicular to the quenching electric field. The question of polarization of quenched Lyman- α radiation has introduced difficulties when trying to compare data from past experiments on H(2s) formation.²³ The effect can be large; assuming the atoms enter the quench field adiabatically, Sellin *et al.*²⁴ have calculated a polarization of -56% at 600 V/cm. In order to avoid this problem the quench radiation in the present experiment was viewed at $\theta = 54.7^\circ$ to the electric field direction. In this case the emitted radiation is independent of polarization since $\cos^2\theta = \frac{1}{3}$ and $I(\theta) = I_0/(4\pi)$.

The quench electric field was applied across two parallel plates 2.4 cm long and separated by 3.9 cm. Electric field fringe effects were significantly reduced by a set of image plates located 3 mm behind the quench plates and extending 3 mm beyond the front edge. The image plates also extended 2.6 cm beyond the downstream edge of the inner plates. This arrangement reduced the net deflection of the primary H⁺ beam to less than one degree at our lowest energy and ensured complete collection of the primary beam during the application of the quench voltage. The magnitude and direction of the quench electric field were obtained from a field mapping simulation of the experimental quench region. By this technique it was determined that in the region where the effective Lyman- α radiation was emitted, the electric field was uniform to within ~10%.

The Lyman- α detector was a channeltron electron multiplier.²⁵ The output signal from the detector was amplified and discriminated, and pulses from individual photons were counted. The photocathode of the detector was coated with

cesium iodide to increase the quantum efficiency for Lyman- α radiation. (Manufacturer specifications indicate that the quantum efficiency is maximum for Lyman- α radiation and is equal to 23%.) Attached to the front of the channeltron was a 2-mm-thick lithium fluoride window which screened the channeltron from stray charged particles and provided a short-wavelength cutoff at 1080 Å. The CsI photocathode surface provided a long-wavelength cutoff at 1800 Å. A grounded mesh was placed on the outer surface of the lithium fluoride window to prevent excess charge buildup and to reduce field penetration.

The photocathode of the Lyman- α detector was 7 cm from the beam axis and viewed a 5-cm-long beam path over which the solid-angle acceptance efficiency changed by less than 8%. This geometrical arrangement resulted in a rather small (<4%) velocity-dependent correction to the Lyman- α signal since in a field of 600 V/cm the maximum decay length of H(2s) atoms in the present experiment was 2 cm. The Lyman- α signal was studied as a function of the applied voltage to the quench plates and saturation of the signal was evident over a range of several hundred volts.

Since the Lyman- α detector viewed a region which was substantially larger than the transverse extent of the beam, minor differences in spatial scattering of the H(2s) atoms using Ar, Mg, and Ba targets are negligible and have no measurable effect on the detector efficiency. Also, based on our knowledge of the electric field in the quench region obtained from the mapping simulation, we conclude that the electric field quenching of H(2s) atoms before the field of view of the detector is negligible. Furthermore, with a pressure of 5×10^{-7} torr in the drift region and assuming an H(2s) collisional destruction cross section of order 10^{-15} cm², the probability of collisional loss of H(2s) prior to detection is of order 10^{-3} , which is negligible. This was demonstrated experimentally by varying the pressure in the drift region and verifying that no change in the Lyman- α signal occurred.

The Lyman- α signal was measured with different polarities on the quench plates and no change in the data was observed. This experimental check demonstrated that several possible sources of error were negligible, including effects caused by the small deflection of the primary H⁺ beam, Lyman- α emission from surfaces due to electron bombardment, and possible detector focusing effects due to the presence of the quench field. All surfaces in the quench region were coated with colloidal graphite to reduce the reflection of Lyman- α photons and to diminish the production of Lyman- α radiation by fast-electron impact on

the surfaces.

With the quench plates grounded, a small background radiation existed of magnitude typically <5% of the signal with the voltage applied. The background signal arose predominantly from collisions of the primary H^+ beam with the ambient gas in the quench region. (Background signal due to the channeltron dark current was completely negligible.) The true $H(2s)$ signal was obtained from the difference in photon counts with the quench voltage applied and with the quench plates grounded.

C. Data analysis

For an incident proton beam of current I^+ the equivalent current of $H(2s)$ atoms counted by the detection system under single-collision conditions with a target thickness of Π atoms/cm² is given by

$$I(2s) = \frac{1}{4}(\omega\epsilon/\pi)(\sigma_{+m}\Pi I^+), \quad (4)$$

where ω is the solid angle viewed by the detector and ϵ is the photon detection efficiency. Using the tabulated value of $\sigma_{+m} = 2.8 \times 10^{-17}$ cm² for $H^+ + Ar$ collisions at 30 keV,¹⁷ we obtained the quantity $\frac{1}{4}\omega\epsilon/\pi$ from the slope of the linear portion of the measured $I(2s)$ vs Π data. For Mg and Ba targets σ_{+m} was then determined from similar measurements. Approximately 20 datum points were measured as a function of Π for each σ_{+m} determination. As a check on our measured overall detection efficiency $\frac{1}{4}\omega\epsilon/\pi$, we estimated the efficiency based on calculated solid angles and the manufacturers' quotations of the channeltron photocathode quantum efficiency and of the Lyman- α transmission coefficient of LiF. The estimated value was within 25% of the results obtained by normalizing the signal to $H^+ + Ar$ collisions at 30 keV.

The reproducibility of σ_{+m} was $\pm 12\%$ over a period of several months. We have assigned a relative uncertainty of $\pm 15\%$ to the data. The absolute uncertainty of the data is more difficult to assess owing to possible systematic errors associated with the calibration of the Lyman- α detector in terms of σ_{+m} in Ar and in the evaluation of the metal vapor pressure from thermodynamic data. We estimate the overall uncertainty in the absolute value of our data to be approximately $\pm 35\%$.

The effect of cascade contributions from $n \geq 3$ states to the observed Lyman- α emission is unknown since there exists almost no information on capture into $n \geq 3$ states using metal-vapor targets. No estimate of the effect of cascade transitions is made in the present work. However, we note that

cascade effects have been estimated to be $\sim 10\%$ in atomic hydrogen²² and 5% in gases²⁶ over the present energy range.

III. RESULTS AND DISCUSSION

In order to verify the reliability of our apparatus and experimental procedure we measured the cross section σ_{+m} in Ar gas over the energy range 3–70 keV. This measurement served as a sensitive test of the Lyman- α detection system since the cross section has both a maximum and a minimum in the energy range studied. It can be seen from Fig. 2 that the present results are in good agreement with the data of Bayfield.¹⁷ There are several other experimental determinations of σ_{+m} in Ar which we have not included in Fig. 2.^{23,26–28} The general shape of the cross section is reproduced by all previous measurements. However, discrepancies do exist in previous results at low energies, and the present data tend to support the measurements of Bayfield. At high energies, the present results are in better agreement with the data of Hughes *et al.*²⁶

Figure 3 shows the present results for σ_{+m} in Mg and Ba vapors. We are aware of no previous experimental or theoretical data with which to compare the present results. However, Berkner *et al.*²⁹ have measured the cross section for electron capture into the $n=6$ state for $H^+ + Mg$ collisions, and we have included their data in Fig. 3. The present results and those of Berkner *et al.* are the only available information on electron

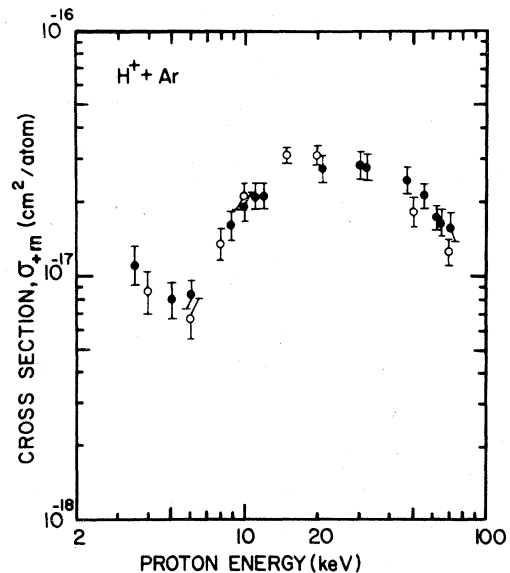


FIG. 2. Cross sections for the formation of $H(2s)$ atoms in $H^+ + Ar$ collisions. Solid circles represent present data, open circles represent data of Ref. 17.

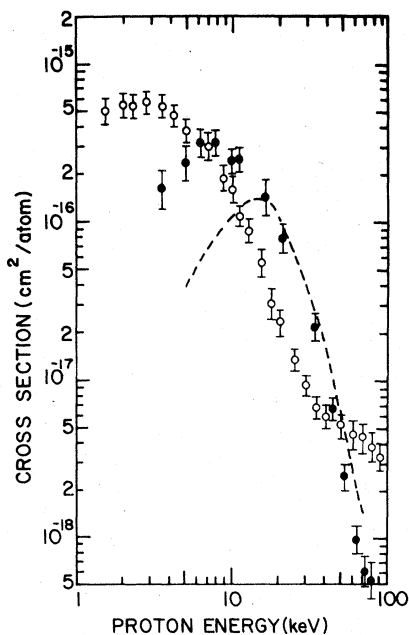


FIG. 3. Cross sections for proton collisions with Mg and Ba. Mg target: solid circles represent present experimental results for $H(2s)$ formation; the dashed curve represents Ref. 29 data for $n=6$ capture (multiplied by ten). Ba target: open circles represent present experimental results for $H(2s)$ formation.

capture into specific hydrogen-atom principal quantum states for $H^+ + Mg$ collisions.

High-velocity Oppenheimer-Brinkman-Kramers theory for electron capture predicts a rough n^{-3} dependence.³⁰ A comparison of the $n=2$ and $n=6$ capture cross sections shown in Fig. 3 for energies greater than 15 keV (which corresponds to impact velocities greater than the orbital velocity of the active electron) indicates that the n^{-3} scaling law is not obeyed. A possible explanation for this disagreement with theory is the failure of the n^{-3} rule for small n . For a given collision system the range over which the rule is applicable is still an open question. However, high-energy experimental evidence exists which supports the n^{-3} law in several gases down to $n=2$.²⁶ A comparable study to test the n^{-3} prediction in metal vapors is needed.

Low-energy behavior in asymmetric charge-transfer collisions into specific quantum states can be discussed in terms of the velocity v_m at which the single-electron-capture cross section reaches a maximum value. Using the Born approximation, Drukarev³¹ has shown that when the energy defect of the collision is small compared to the ionization potential of the target, i.e., $|\Delta E_\infty| \ll I$, the relation $v_m \propto |\Delta E_\infty|$ is valid, in agreement with the Massey adiabatic criterion.³² However,

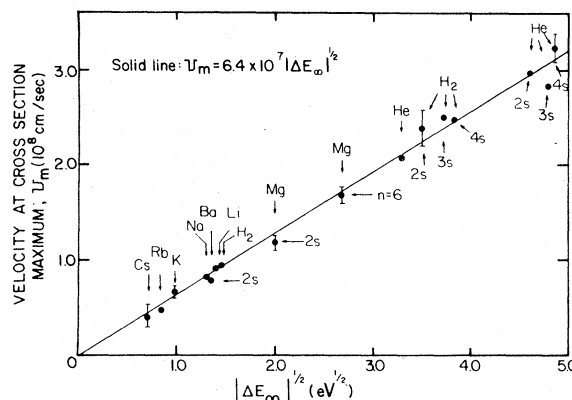


FIG. 4. Velocity at the electron-capture cross section maximum v_m as a function of $|\Delta E_\infty|^{1/2}$ for ns^1 and ns^2 targets. The data shown are experimental results taken from the present work and from Ref. 34. Representative error bars are indicated.

for the present case of capture into the $2s$ state using Mg and Ba, the relation $|\Delta E_\infty| \sim I$ is a much better approximation. For this case the analysis of Drukarev predicts the relation $v_m \propto |\Delta E_\infty|^{1/2}$. We find that within experimental error the relation $v_m \propto |\Delta E_\infty|^{1/2}$ is satisfied for capture into the $2s$ state in Mg and Ba targets. The corresponding analysis based on the Massey criterion predicts a maximum-velocity ratio in excess of twice the measured value. Similar conclusions have been obtained for total single-electron capture in alkali-metal vapors.³³

In Fig. 4 we plot v_m as a function of $|\Delta E_\infty|^{1/2}$ for available alkali (ns^1)- and alkaline-earth (ns^2)-metal-vapor targets. We have also included in the figure helium and molecular hydrogen. Helium represents the first member of the alkaline-earth sequence, and H_2 may be considered as a member of either sequence. The data plotted in Fig. 4 include total electron capture (into all n states) and capture into well-defined states.³⁴ In the case of Cs, Rb, K, Na, and Li total cross sections were measured and we have assumed capture occurs primarily into $n=2$ states. Total cross sections in He and H_2 have been interpreted as being due to capture into the ground state of hydrogen. Post-collision excited states of hydrogen are indicated in the figure for Ba, Mg, H_2 , and He targets. The result shown in Fig. 4 is quite striking and strongly supports the relation $v_m \propto |\Delta E_\infty|^{1/2}$ for ns targets, even for those cases in which $|\Delta E_\infty| \sim I$ is apparently not a valid approximation, e.g., capture into excited states for H_2 and He targets.

Olson³⁵ has derived an expression for the velocity at the cross section maximum for charge transfer at large internuclear separations where the potential curves lie parallel to one another. His result

is

$$v_m = 14.5 \times 10^7 |\Delta E_\infty| / I^{1/2}, \quad (5)$$

where v_m is in cm/sec and $|\Delta E_\infty|$ and I are in eV. As noted by Olson, this result is intended only as a guide since several convenient approximations were made to derive the formula. Substituting $|\Delta E_\infty| \sim I$ into Eq. 5, we obtain

$$v_m = 14.5 \times 10^7 |\Delta E_\infty|^{1/2}, \quad (6)$$

which is in reasonably good agreement with experiment (see Fig. 4) considering the nature of the approximations.

Our results for the metastable fraction of the neutral beam, f , due to electron capture in H^+ collisions with Mg and Ba atoms are shown in Fig. 5. These results were obtained by taking the ratio of the cross section for capture into the $2s$ state, σ_{+m} , relative to the total capture cross section σ_{10} . Both cross sections were measured simultaneously and σ_{10} has been reported in Ref. 18. Also shown in Fig. 5 is our evaluation of f at 100 keV based on the Brinkman-Kramers results of Hiskes.³⁶ As can be seen from the figure, reasonable agreement is found. For comparison we have included in the figure recent determinations

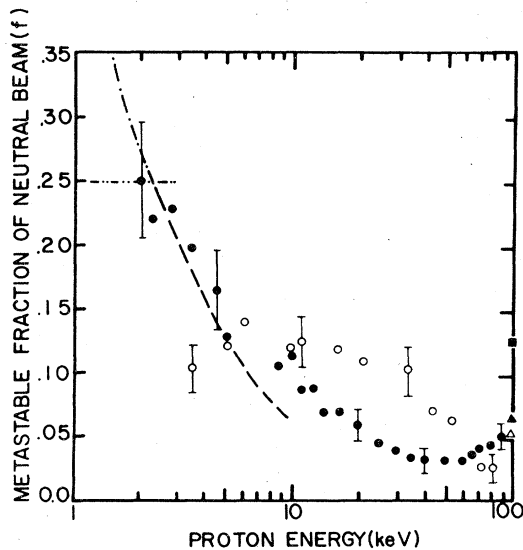


FIG. 5. $H(2s)$ metastable atom fraction f of the neutral beam as a function of proton energy for Cs, Mg, and Ba thin targets. Cs target: --- represents the results of Ref. 20; —•—, Ref. 12; —••—, Ref. 13; solid square at 100 keV, present evaluation of f based on Brinkman-Kramers (BK) results of Ref. 36. Mg target: open circles represent present experimental results; open triangle at 100 keV, present evaluation of f based on BK results of Ref. 36. Ba target: solid circles represent present experimental results; solid triangle at 100 keV, present evaluation of f based on BK results of Ref. 36.

of f for a Cs target. In this case the maximum value of f is below 1 keV and has been reported as 0.43 ± 0.03 at 0.5 keV,¹³ and 0.55 ± 0.075 at 0.6 keV.¹² Although it was not expected that the metastable fraction would reach such large values for Ba, the present results indicate that an investigation at lower energies would be interesting.

In the case of Ba, the rise in the metastable fraction of the neutral beam at high energies (see Fig. 5) is due to the fact that σ_{+m} decreases less rapidly with energy than σ_{10} for energies greater than 50 keV. As can be seen from Fig. 3 the cross section σ_{+m} in Ba shows an abrupt change in energy dependence at 30 keV. This behavior is more clearly illustrated in Fig. 6, where we have graphed σ_{+m} as a function of energy on a semilog plot. Also, as can be seen from Fig. 6, σ_{+m} in Mg exhibits an abrupt change in energy dependence, but at a higher energy. This behavior is attributed to inner core effects and is consistent with theoretical prediction. A discussion of the comparison between theory and experiment for the onset of inner-shell capture in Mg and Ba has been recently presented by Morgan and Eriksen.¹⁸ For comparison with the present results we have plotted in Fig. 6 the cross section σ_{+m} for He and Ar targets.²⁶ The high-energy dependence for all targets in Fig. 6 is similar and is attributed to

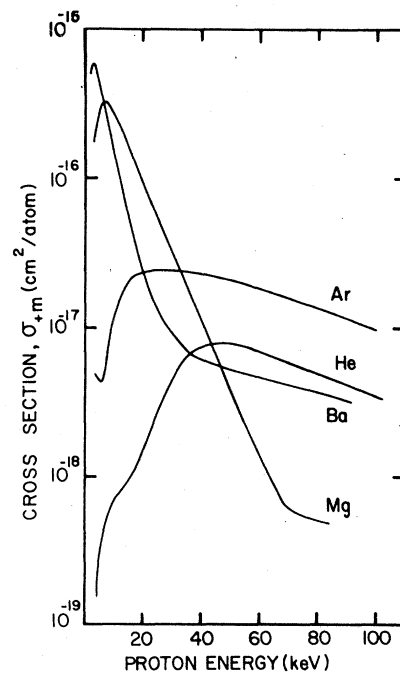


FIG. 6. Cross section for the formation of $H(2s)$ atoms in Ar, He, Ba, and Mg targets. The Ar and He data have been taken from Ref. 26. The Mg and Ba data are present results.

capture of electrons from closed shells of the target. The relative magnitude of the cross section at high energy for all targets shown in Fig. 6 is consistent with energy-defect arguments, assuming the electron is captured from the outermost closed shell of the target. As the energy decreases, σ_{+m} in Mg and Ba rises abruptly owing to capture of electrons from the valence shell via

radially and/or rotationally induced transitions.^{15, 37} Since He and Ar are closed-shell structures, σ_{+m} does not exhibit this steep rise at low energies in these gases.

ACKNOWLEDGMENT

This work was supported by the Research Corporation and the U. S. Department of Energy.

*Present address: Dept. of Physics, Univ. of Southern Mississippi, Hattiesburg, Miss. 39401.

- ¹B. L. Donnally and W. Sawyer, *Phys. Rev. Lett.* **15**, 439 (1965).
²D. Hennies, R. S. Raymond, L. W. Anderson, W. Haerberli, and H. F. Glavish, *Phys. Rev. Lett.* **40**, 1234 (1978).
³R. Ptak and R. Stoner, *Nature (London)* **24**, 280 (1973).
⁴J. W. McGowan and R. F. Stebbings, *Appl. Opt. Suppl.* **2**, 68 (1965).
⁵P. A. Bokhan and V. I. Solomonov, *Kvantovaya Elektron.*, (Moscow) **5**, 319 (1978) [*Sov. J. Quantum Electron.* **8**, 184 (1978)].
⁶H. B. Gilbody, in *Proceedings of Conference on Atomic Collision Processes: A Conference in Honor of Sir Harrie Massey*, University College, London, 1978 (to be published).
⁷A. Johannessen and D. Krankowsky, *J. Geophys. Res.* **77**, 2288 (1972); R. S. Narcisi and A. D. Bailey, *ibid.* **70**, 3687 (1965).
⁸B. L. Donnally, T. Clapp, W. Sayer, and M. Schultz, *Phys. Rev. Lett.* **12**, 502 (1964).
⁹A. Cesati, F. Cristofori, L. Millazo Colli, and P. G. Sona, *Energ. Nucl. (Milan)* **13**, 649 (1966).
¹⁰I. A. Sellin and Granoff, *Phys. Lett. A* **25**, 484 (1967).
¹¹G. Spiess, A. Valance, and P. Pradel, *Phys. Rev. A* **6**, 746 (1972).
¹²P. Pradel, F. Roussel, A. S. Schlachter, G. Spiess, and A. Valance, *Phys. Rev. A* **10**, 797 (1974).
¹³Vu Ngoc Tuan, G. Gautherin, and A. S. Schlachter, *Phys. Rev. A* **9**, 1242 (1974).
¹⁴A. Valance and G. Spiess, *J. Chem. Phys.* **63**, 1487 (1975).
¹⁵R. E. Olson, E. J. Shipsey, and J. C. Browne, *Phys. Rev. A* **13**, 180 (1976).
¹⁶V. Sidis and C. Kubach, *J. Phys. B* **11**, 2687 (1978).
¹⁷J. E. Bayfield, *Phys. Rev.* **182**, 115 (1969).
¹⁸T. J. Morgan and F. Eriksen, *Phys. Rev. A* **19**, 1448 (1979).
¹⁹T. Nagata, *Phys. Lett. A* **56**, 261 (1976).
²⁰F. Brouillard, W. Claeys, and G. Van Wassenhove, *J. Phys. B* **10**, 687 (1977).

- ²¹R. R. Hultgren, P. O. Dlsai, D. T. Hawkins, M. Gleiser, K. K. Kelly, and D. D. Wagman, *Selected Values of Thermodynamic Properties of the Elements* (American Society for Metals, Cleveland, Ohio, 1973).
²²T. J. Morgan, J. Geddes, and H. B. Gilbody, *J. Phys. B* **6**, 2118 (1973).
²³R. L. Fitzwilson and E. W. Thomas, *Phys. Rev. A* **3**, 1305 (1971).
²⁴I. A. Sellin, J. A. Biggerstaff, and P. M. Griffin, *Phys. Rev. A* **2**, 423 (1970).
²⁵Galileo Electro-Optics Corporation, Sturbridge, Massachusetts.
²⁶R. H. Hughes, E. D. Stokes, Song-Sik Choe, and T. J. King, *Phys. Rev. A* **4**, 1453 (1971).
²⁷D. Jaecks, B. van Zyl, and R. Geballe, *Phys. Rev.* **137**, A340 (1965).
²⁸E. P. Andreev, V. A. Ankudinov, and S. V. Bobashev, *Sov. Phys. JETP* **23**, 375 (1966).
²⁹K. H. Berkner, W. S. Cooper, S. N. Kaplan, and R. V. Pyle, *Phys. Rev.* **182**, 103 (1969).
³⁰J. D. Jackson and H. Schiff, *Phys. Rev.* **89**, 359 (1953).
³¹G. F. Drukarev, *Sov. Phys. JETP* **25**, 326 (1967).
³²H. S. W. Massey and E. H. S. Burhop, *Electronic and Ionic Impact Phenomena* (Oxford University, London, 1956), Chap. VII, p. 441.
³³W. Gruebler, P. A. Schmelzbach, V. Konig, and P. Marmier, *Helv. Phys. Acta.* **43**, 254 (1970).
³⁴Other than the present results, the cross-section data used to prepare Fig. 4 have been taken from the following sources: Ref. 29; and Ref. 33; R. J. Girnius, L. W. Anderson, and E. Staab, *Nucl. Instrum. Methods* **143**, 505 (1977); J. F. Williams, *Phys. Rev.* **157**, 97 (1967); R. H. Hughes, E. D. Stokes, Song-Sik Choe, and T. J. King, *Phys. Rev. A* **4**, 1453 (1971); R. H. Hughes, C. A. Stigers, B. M. Doughty, E. D. Stokes, *ibid.* **1**, 1424 (1970); R. H. Hughes, H. R. Dawson, and B. M. Doughty, *Phys. Rev.* **164**, 166 (1967).
³⁵R. E. Olson, *Phys. Rev. A* **6**, 1822 (1972).
³⁶J. R. Hiskes, Lawrence Livermore Laboratory Report UCRL-50602, 1969 (unpublished).
³⁷A. Russek, *Phys. Rev. A* **4**, 1918 (1971).